

SCIENTIFIC REPORTS



OPEN

Fabrication and Verification of Conjugated AuNP-Antibody Nanoprobe for Sensitivity Improvement in Electrochemical Biosensors

Patricia Khashayar^{1,2,3}, Ghassem Amoabediny^{4,5}, Bagher Larijani⁶, Morteza Hosseini¹ & Jan Vanfleteren²

This study was designed to obtain covalently coupled conjugates as means for achieving higher stability and better coverage of the AuNPs by antibodies on the particle surface suitable for sensor performance enhancement. Starting by using a modified protocol, colloid gold solution, with mean AuNP core size of ~6 nm was synthesized. The protocol used for conjugation of AuNPs to osteocalcin antibody in this study relies on covalent and electrostatic attractions between constituents. Varieties of conjugates with varying combinations of crosslinkers and different concentrations were successfully synthesized. The obtained products were characterized and their properties were studied to determine the best candidate in sense of antibody - antigen reactivity. Using AuNP-GSH-NHS-Ab combination (1:1:1), the tertiary structure of the protein was maintained and thus the antibody remained functional in the future steps. This one-pot method provided a simple method for covalently coupling antibodies on the particle surface while keeping their functionality intact. The AuNP content of the solution also accelerated electron transfer rate and thus amplifies the detection signal. With the developed and discussed technique herein, a simple solution is modeled to be used for measuring serum levels of biomarkers in single and/or multiplexed sensor systems.

Designing sensors with higher efficiency depends on the development of novel materials to improve both the recognition and transduction steps. Studies have shown that labeling biomolecules with noble metal NPs results in highly sensitive and specific bioassays, while maintaining the bioactivity of the biomarker¹⁻³. Such NPs can also help improve signal detection for low concentration of analytes.

Gold nanoparticles (AuNPs) are the most commonly used labels in sensor studies because of their intriguing size dependent electrical, optical, magnetic, and chemical properties as well as their ease of synthesis and surface functionalization^{4,5}. Being redox active, AuNPs provide the possibility for miniaturizing the sensing devices to nanoscales, offering excellent prospects for chemical and biological sensing. They also provide a suitable platform for multifunctionalization with a wide range of organic or biological ligands for selective detection of biomarkers⁶.

As a result, broad potential of AuNPs for signal amplification in antibody (Ab) - antigen (Ag) reaction events on simple, ultrasensitive, multiplexed immunosensors become apparent⁷. AuNP conjugation with different proteins is well studied in the literature but the mechanisms behind the process are poorly understood⁸⁻¹¹. Therefore, special attention is needed to ensure the quality of the end product. Different protocols were thus tested in this

¹Nanobiotechnology Department, Faculty of New Sciences & Technologies, University of Tehran, Tehran, Iran. ²Center for Microsystems Technology, imec and Ghent University, Gent-Zwijnaarde, Belgium. ³Osteoporosis Research Center, Endocrinology and Metabolism Clinical Sciences Institute, Tehran University of Medical Sciences, Tehran, Iran. ⁴Department of Biotechnology, Faculty of Chemical Engineering, School of Engineering, University of Tehran, Tehran, Iran. ⁵Nanobiotechnology Department, Research Center for New Technology in Life Sciences Engineering, University of Tehran, Tehran, Iran. ⁶Endocrinology and Metabolism Research Center, Endocrinology and Metabolism Clinical Sciences Institute, Tehran University of Medical Sciences, Tehran, Iran. Correspondence and requests for materials should be addressed to G.A. (email: amoabediny@ut.ac.ir) or J.V. (email: jan.vanfleteren@imec.be)

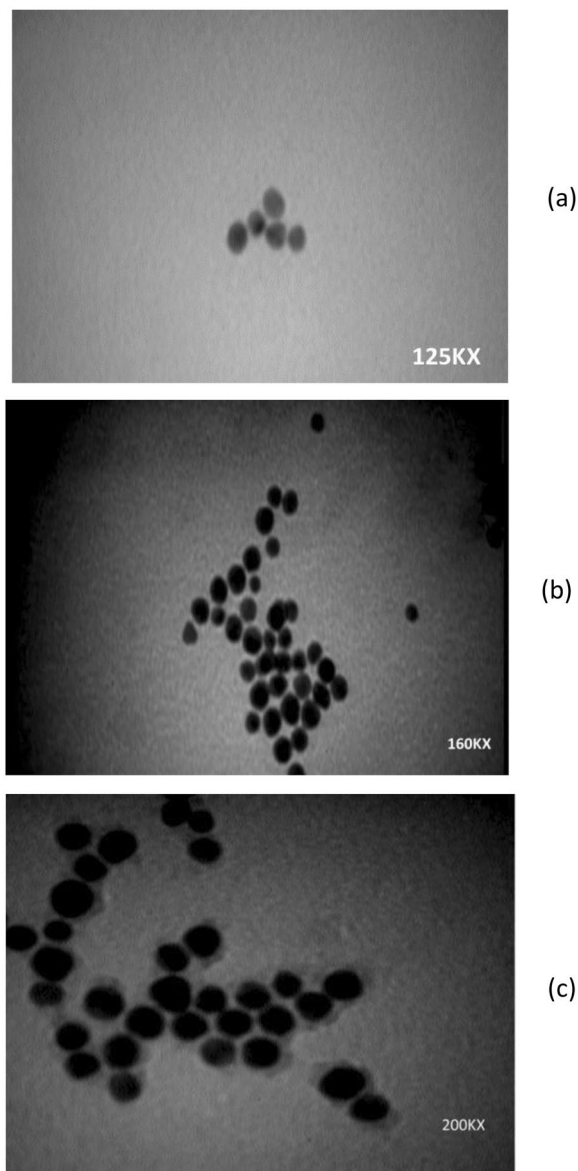


Figure 1. TEM results. (a) Monodispersed gold nanoparticles, (b) Gold nanoparticles capped with GSH, (c) Antibody- conjugated gold nanoparticles (With permission)¹³.

study to confer a controlled immobilization of antibody on the surface, while maintaining the activity of the bounded antibody. With the developed and discussed technique herein, a simple solution has been modeled to be used for measuring serum levels of biomarkers in single and/or multiplexed sensor systems^{12,13}.

Results and Discussion

Characterization of AuNPs. The sodium citrate in the AuNP preparation procedure behaves as a reducing agent. It also provides the negative surface charge around the AuNPs, needed to repel the particles and restrain any aggregation. The concentration of gold salt and trisodium citrate as well as the temperature and mixing rate are main factors defining the size-distribution of the synthesized colloidal gold nanoparticles¹⁴.

In this work, TEM was used to characterize the morphology and determine the size of the as-prepared AuNP solution. According to the ImageJ results, uniformly distributed, mainly spherical, nanoparticles with an average size of 6.53 ± 1.8 nm were observed in the solution with very few particles of higher and lower size distribution (Fig. 1).

The mean hydrodynamic diameter of the nanoparticles, suggestive of the mean diameter of the majority of the particles according to number (%) was measured using a zeta-sizer nano-ZS (Fig. 2). As expected, the DLS values were larger than those reported by TEM (7.48 nm vs. 6.53 nm) due to the presence of the double layer effect in the calculations of the hydrodynamic radius of the particles in the solutions, and its absence in that of the dried-state samples imaged by TEM. Moreover, DLS results are quite dependent on the viscosity and temperature.

Assuming a spherical shape and a uniform FCC crystal structure, the average number of gold atoms per nanoparticle (N) was calculated using the following equation (eq. 1) and based on TEM findings:

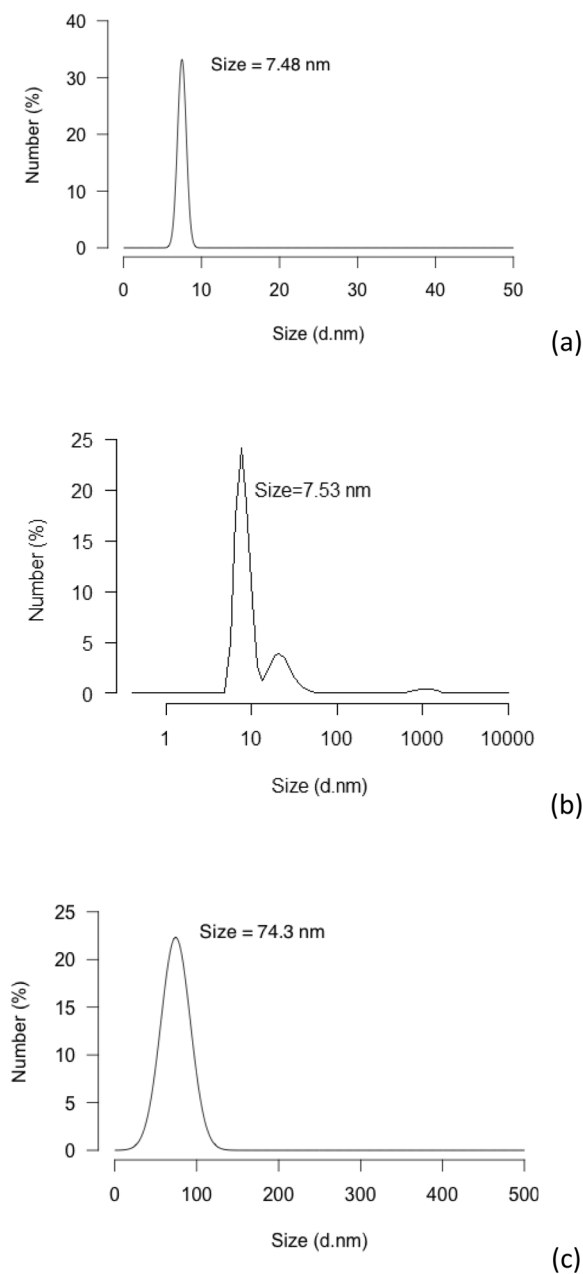


Figure 2. DLS results. (a) Gold nanoparticles, (b) Gold nanoparticles capped with GSH, (c) Ab-conjugated gold nanoparticles (with Permission)¹³.

$$N = \frac{\pi \rho D^3}{6 M} = 8594 \quad (1)$$

where D is the average core diameter of the particles (nm), ρ is the density for fcc gold (19.3 g/cm^3), and M stands for the atomic weight of gold (197 g/mol)¹⁵.

Then the molar concentration of the nanosphere solution was calculated by dividing the total number of gold atoms (N_{total} = initial amount of gold salt added to the reaction solution) by the average number of gold atoms per nanosphere (N), using the following equation (eq. 2):

$$C = \frac{N_{\text{Total}}}{NVN_A} = 1.96 * 10^{-6} \text{ mol/L} \quad (2)$$

The properties of the prepared AuNP solution were also determined through calculation of its extinction coefficient as well as the absorption peak and curve appearance. The UV-Vis spectrophotometer has been the first optical technique employed for this regard. In this method, the width of the absorption spectra is related to the size distribution range of the nanoparticles; as a result, the absorption peak shifts to longer wavelengths with

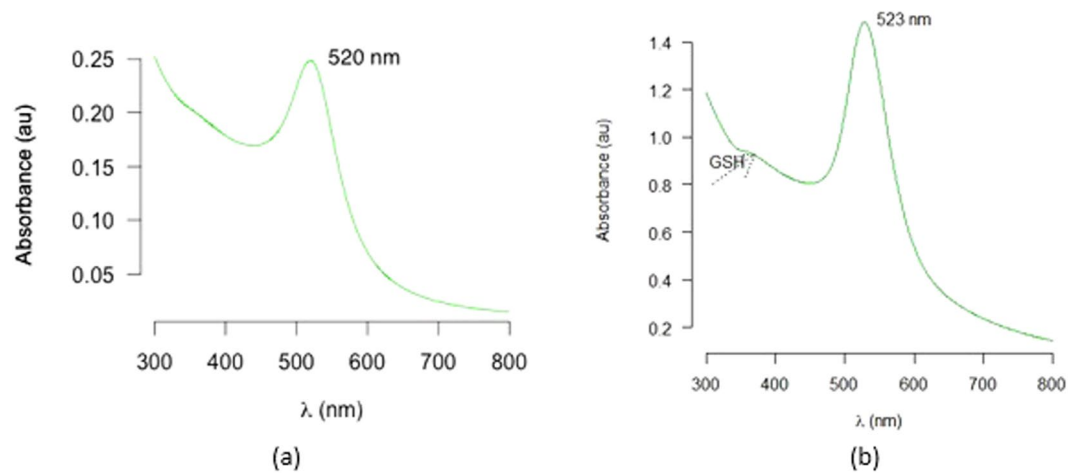


Figure 3. UV-Vis spectra of (a) colloidal AuNPs (b) GSH-capped AuNPs.

increasing particle size. In the present study, the plasmon absorption peak was observed at ~ 520 nm, which is corresponding to the typical surface plasmon resonance (SPR) of colloidal AuNPs prepared by the conventional citrate reduction method (Fig. 3)¹⁶. Lack of a band at around 680 nm indicated the absence of aggregated gold particles and thus confirmed the successful preparation of an AuNP solution¹⁷.

The Lambert-Beer law was used to calculate the extinction coefficient, the sum of absorption and scattering coefficients (ϵ), of the nanoparticle solution (eq. 3).

$$A = \epsilon bC \rightarrow \epsilon = 2.65 * 10^8 M/cm \quad (3)$$

Where A is the absorbance at 520 nm, b is the length of solution that the light passes through (cm) and C is the concentration of the solution (mol/cm^3).

It should be noted that the calculated extinction coefficient of our colloid solution was higher than the solutions made using the same technique in the literature ($8.56 * 10^6$ or $5.14 * 10^7$)¹⁵.

AuNP/Ab nanocomplex. This study was designed to obtain covalently coupled conjugates as means for achieving higher stability and better coverage of the AuNPs by antibodies on the particle surface suitable for sensor performance enhancement. GSH is a tripeptide biomolecule (-Glu-Cys-Gly), containing a -SH group which can easily be adsorbed onto the AuNP surface. A dense layer of GSH-AuNP enlarges the electroactive surface area and provides carboxylic groups for covalently binding of the particles to a dense layer of antibody/protein for detection. EDC and sulfo-NHS, on the other hand, acted as cross-linkers facilitating the bonding of an amine group of the antibody to the carboxylic group of GSH.

In other words, using this combination, the binding of antibody complex to gold atoms happened through thiol linkages as well as ionic interactions between the negatively charged gold surface and the positively charged terminals on the complex, along with interactions originating from absorption of hydrophobic groups on AuNPs (Fig. 4). This is while the conjugates developed through direct absorption of the antibody on the surface of the nano-colloid particles using non-covalent bonds, such as London-van der Waals force and hydrophobic interactions, are reported not to be stable^{18,19}.

Functionality of AuNP/Ab nanocomplex. As mentioned earlier, the final goal in the sensor development process is to maintain the bioactivity and functionality of the antibody immobilized on the electrode surface. In this regard, various techniques are reported in the literature^{20–22}. Our results revealed that using AuNP-GSH-NHS-Ab combination (1:1:1), the tertiary structure of the protein was maintained and thus the antibody remained functional in the future steps. This was confirmed based on a significant decrease noted in the maximum peak after the antigen was left to react with the electrode modified with the 1:1:1 GSH-NHS-Ab nanoconjugate for at least 2 hours. The reason behind the noted decrease in the measured current is the fact that the binding of antigen to the immobilized antibody disrupts electron transfer.

As for the rest, a minimum change from baseline value ($<3\%$) was reported, indicating that the antibody bounded using those protocols either had lost its activity or did not have the correct orientation (Fig. 5). In other words, the conjugates were found not to be functional in the presence of EDC; this could be explained by the fact that EDC may resemble hydroxyapatite effects and thus alter the tertiary structure of the osteocalcin²³.

Another advantage of the abovementioned method was that covalent coupling via a cross-linker is specific and controllable. Thus, the nanocomplex prepared using this protocol is going to be discussed in the rest of this article.

Characterization of AuNP/Ab nanocomplex. Characterization of the resulting conjugates was done by TEM measurements of freshly prepared solution (Fig. 1). GSH molecules are believed to form certain intermolecular hydrogen binding among themselves, even when they are adsorbed on AuNPs²⁴. The concentration ratio of GSH and AuNP, thus, is one of the important factors that affects the aggregation rate in the solution. According to our results, no aggregates were formed upon the addition of GSH to the AuNP solution. UV-Vis confirmed the

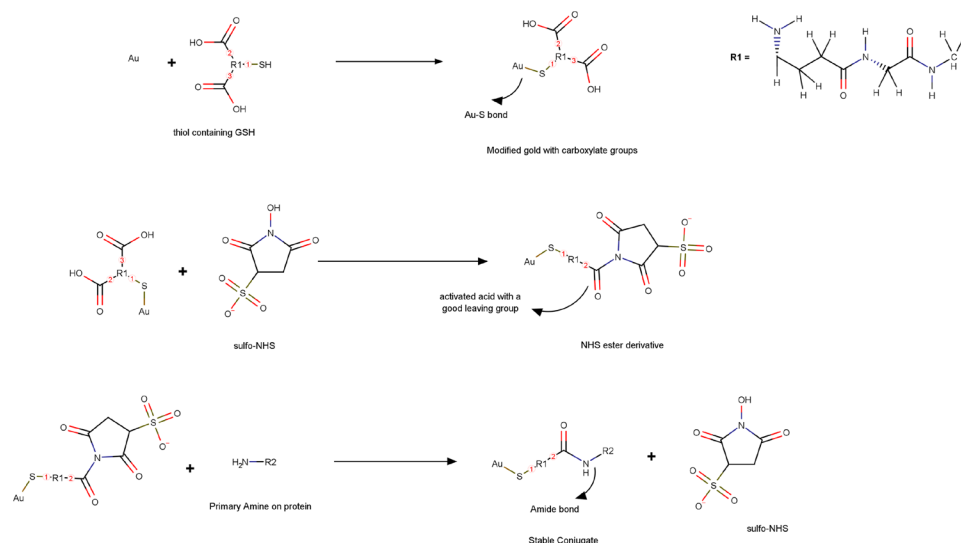


Figure 4. Representative schematic showing nanoconjugate formation steps.

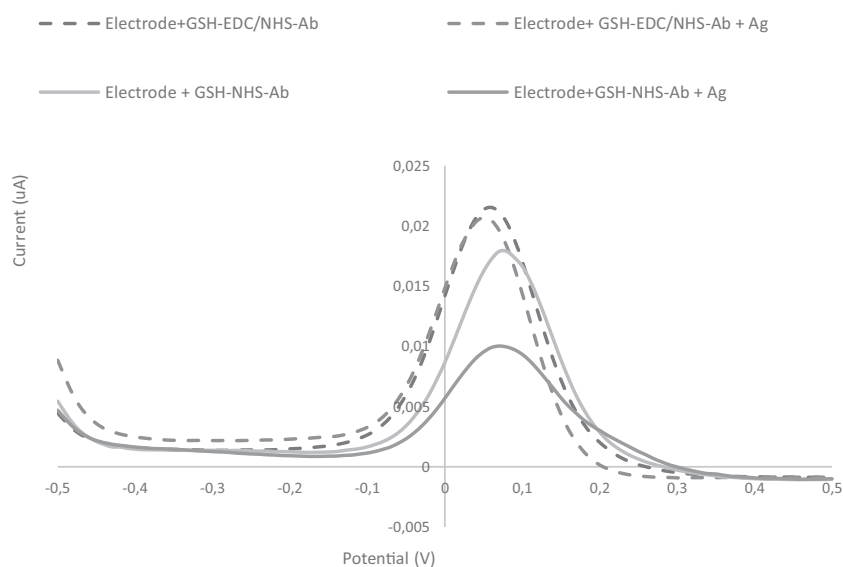


Figure 5. DPV plots of two different nanoconjugates before and after reaction with antigen (Ag) for 2 hrs.

successful formation of GSH-capped AuNPs; and the absence of any significant alteration in particle morphology or size, based on TEM and DLS findings, confirmed the latter (Figs 2 and 3).

The attachment of the antibody to GSH-modified gold nanoparticles, on the other hand, resulted in a considerable increase in size and the formation of core-shell structure, which is in accordance with the findings of previous reports^{25,26}. In other words, the size increase confirmed the existence of an additional layer of conjugated antibody on the nanoparticles.

Assuming that the increase in the particle size (diameter) was caused by the NHS-Ab, one could also conclude that this increase is equivalent to the diameter of the monolayer of antibody around the core AuNP. Thus, the volume of the core-shell is calculated as the difference between the antibody-conjugated nanoparticles and the AuNP, given by (eq. 4):

$$V = 0.5236(D^3 - d^3) = 8333.53 \text{ nm}^3 \quad (4)$$

where D is the diameter of the antibody-conjugated nanoparticles and d is the diameter of the core AuNP. By dividing the volume of the core-shell by that of the antibody obtained using the calculated hydrodynamic diameters, it could be concluded that at least 2 antibodies attach to each nanoparticle in this technique.

Nanoparticle colloid is stabilized by the electrostatic forces, indicated by the zeta potential of the particles in solution. This arises due to an energy barrier originating from the balance between two opposing forces: the van der Waals attractive (V_A) and electrical double layer repulsive (V_R) forces between the particles approaching each other²⁷. This barrier prevents the two particles from agglomerating.

Zeta potential is influenced by the thickness of the electrical double layer, the electrical charge in this layer and dielectrical constant²⁸. As a result, the particle's surface charge is an important factor influencing the stability and reactivity of the nanoparticle, and thus can greatly enhance the nanoparticle conjugates' application. In line with the Huckel's theory, our results showed that the zeta potential value increased with particle size, and that the particle charge is directly proportional to the zeta potential.

Optimization of AuNP/Ab nanoconjugate. The preparation of a well-dispersed nanoprobe with uniform size distribution and no aggregation is of great importance in immunoassay studies. Therefore, lowest amount of antibody enough to stabilize the gold was determined by incubating 1 mL of colloid gold with antibody solutions at varying concentrations (1–50 µg/mL, 1 mL) for 5 min. Thereafter, 0.5 mL of 10 % (w/v) NaCl was added and the color of the solution was noted. The concentration in which the color of the solution turned blue was considered as the minimum required amount for stabilization.

Further tests to assess the reactivity of the nanocomplex towards antigen showed that lower concentrations of antibody produced small current change, suggestive of the absence of sufficient amount of antibody to react with the antigen on the surface. Higher concentrations of the nanoprobe, on the other hand, improved the current while contributing to higher nonspecific adsorption.

As mentioned in the literature, environmental factors such as temperature and pH play an important role in the efficiency of the nanoconjugate^{29,30}. Thermal optimum depends on the chemical nature of the protein, adding that hydrogen bonds are more stable at low temperature, whereas the strength of the hydrophobic bonds increases with temperature³¹. Antigen - antibody reactions are also expected to stabilize at lower temperatures. According to our results, however, no significant change was reported when the incubation was performed at a temperature range of 4 °C to room temperature. As a result, to simplify the process, all the processes were performed at room temperature and the optimized incubation time for this temperature, needed for saturated binding of the immunoreaction, was calculated to be 2.5 hours.

The pH of the solution is another factor affecting the quality of the end product. The optimal reaction rate of NHS chemistry proceeds around pH 4.5–7.2. In other words, NHS-esters hydrolyze faster in higher pH, whereas no reaction takes place at pH values lower than 3.5³². As for GSH, best results are achieved by adjusting the pH at values in which the carboxylic groups are in their protonated form. This occurs when GSH is as a zwitterion (pH = 3–7)³³. Moreover, extreme pH values induce marked conformational changes in the Ab molecule that probably may affect its complementarity with the antigen. On the other hand, since osteocalcin, the Ab used in this study, has an isoelectric point (pI) of 4.4, at lower pH values it carries more positive charge and thus positively influences the electrostatic attraction between the oppositely charged surface carboxyl anions and the protonated amino group of the ligand. As a result, no attempts were made to change the negative pH of the sulfo-NHS solution.

Conclusion

Generally, electrochemical sensors have the virtue of high sensitivity and selectivity, but they require several fabrication steps. Through the inherent interaction between AuNPs and antibody biomolecules, a novel gold nanoprobe was developed herein to be used in nonenzymatic electrochemical immunoassays. This one-pot method provides a simple method for covalently coupling antibodies on the particle surface while keeping their functionality intact. The AuNP content of the solution also accelerates electron transfer rate and thus amplifies the detection signal.

The nanoprobe properties depend on particle size, combination and concentration of cross-linker and the Ab on one hand and the immobilization technique on the electrode on the other hand. The main idea of this study was to optimize the nanoconjugate to have an immunologically reactive solution toward the antigen. The next step, thus, would be to optimize the immobilization process of the nanoprobe on the electrode surface. Considering the results, the proposed method shows a promising potential for clinical applications.

Methods

Materials and reagents. Osteocalcin monoclonal antibody (ab13418) and full-length osteocalcin protein (ab152231) were purchased from Abcam Co. (UK) and were reconstituted in phosphate buffered saline (PBS). The latter was purchased in powder form from Sigma-Aldrich Chemical Co. (Belgium) and was used to prepare a working solution of 10 mM phosphate buffer (NaCl 0.138M, KCl 0.0027M), pH 7.4 at 25 °C. Tetrachloroauric acid ($\text{HAuCl}_4 \cdot 3\text{H}_2\text{O}$), sulfo-a-N-hydroxysuccinimide (sulfo-NHS), b-1-ethyl-3-(3-dimethylammonio)propyl carbodiimide (EDC), L-Glutathione reduced (GSH), Bovine Serum Albumins (BSA), Potassium hexacyanoferrate (III) ($\text{K}_3\text{Fe}(\text{CN})_6$) and trisodium citrate were also obtained from Sigma-Aldrich. Distilled water was used throughout the experiments.

Carbon (DRP-110) screenprinted electrodes (SPEs) (DRP-C223AT) were purchased from Dropsens (Spain).

Apparatus. In order to obtain information about structure, morphology and size of the synthesized AuNPs and antibody conjugated AuNPs, UV-Vis spectroscopy, transmission electron microscopy (TEM) analysis, dynamic light scattering (DLS) and zeta potential measurements were applied.

The absorption spectroscopic measurements were recorded using a UV Visible Spectrophotometer SPECORD 250 (Analytik Jena, Japan).

The TEM images were obtained with an EM10C 80 KV (Zeiss, Germany) transmission electron microscope. The samples for TEM measurements were prepared by placing a droplet of the colloidal solution onto a

carbon-coated copper grid and allowed it to dry in air. Using ImageJ software, the average core diameter of the particles were measured.

DLS measurements to determine the size of the particles were carried out using a MALVERN Instrument MAL1001767 UK, at the temperature of 25 °C and pH 7.4. By this method, the dynamics of the particles system in relation with the Brownian motion and fluctuations of scattered light was investigated with time. The frequency shifts, the angular distribution, the polarization, and the intensity of the scatter light were determined by the size, shape and molecular interactions in the scattering material. The Malvern Zetasizer Nano Instrument was also used for all zeta potential measurements.

All electrochemical experiments were performed using a computer-controlled DropSens STAT 400 (DropSens, Spain). They were carried out in a beaker, at room temperature (23 °C), using the three-electrode configuration. Differential Pulse Voltammetry (DPV) was performed to confirm surface modification changes. The DPV cycles were performed in 0.1 mM $K_3[Fe(CN)_6]$, containing 0.01 M NaCl solution, applying following parameters: 0.05 V modulation amplitude, 0.01 s modulation time, 0.01 V step potential and voltage range from -0.5 to 0.5 V.

Synthesis of conjugated AuNP - antibody nanoprobe. — *Synthesis of AuNPs.* In order to synthesize 10–100 nm AuNPs, the Turkevich method improved by Frens was used^{34,35}. Briefly, 200 ml of 0.01 % $HAuCl_4$ solution was brought to boil while stirring gently. Thereafter, 4.5 ml of 1 % trisodium citrate was rapidly added to the boiling solution while stirring constantly for an additional 15 min. Once mixing occurred, the color of the solution changed gradually from light yellow to wine red. The solution was then cooled down to room temperature. This solution was stored at 4 °C for further use.

Synthesis of GSH-capped AuNPs. A stock solution of glutathione (10 mM) was prepared. Dilute HCl solution (10 mM, 100 mL) was added to colloidal AuNP solution (3 mL) to lower the pH (~4)³⁶. An aliquot of GSH solution (10 mM, 30 mL) was added to the acidic gold solution. This was the maximum amount required before the color of the solution changed from deep red to blue, indicating formation of aggregates amongst AuNPs.

Synthesis of AuNP - antibody Conjugates. A design of experiments (DOE) was prepared to assess the role of various parameters (different crosslinker combinations and concentration ratios) in manufacturing the AuNP - Ab conjugates, which would result in the best performance for the nanoprobe. The four parameters studied were the EDC (0, 100 mM, 200 mM, and 400 mM), sulfo-NHS (0, 100 mM, 200 mM and 400 mM), GSH (0, 10 mM) and Ab concentrations (10 µg/mL and 20 µg/mL). In other words, different concentration ratios of these material were combined to fabricate the nanoconjugate.

In each protocol, specific concentrations of the freshly prepared EDC and sulfo-NHS solutions were mixed and left to react for half an hour. Then the Osteocalcin antibody was added to the solution and incubated for 2.5 hours. The complex was finally added to the GSH-capped AuNP solution and left to react for another hour. After each step, the solution was mixed using a fixed-speed vortex mixer. All the above mentioned procedures, mixing and incubating, was done at room temperature.

Functionality of AuNP/Ab nanocomplex. The reactivity of the AuNP/Ab nanoconjugates prepared using different protocols was tested using osteocalcin protein, herein referred to as the antigen (Ag). This was done by dropping 3 µL of the AuNP/Ab nanoconjugates on a gold SPE and waiting for an hour to dry. 20 µL of 0.2% BSA solution in PBS buffer was added to block the unreacted active functional groups. The electrode was then rinsed for 3 min with 0.1 M PBS to eliminate non-specific bindings. The baseline DPV plots were then recorded in 0.1 mM $K_3[Fe(CN)_6]$ for each nanoconjugate.

Thereafter 3 µL of the Osteocalcin antigen was dropped on the modified electrodes and left to react for 0.5, 1, 2, 5, 10 and 20 hours. The second DPVs were then plotted.

References

- Arruebo, M., Valladares, M. & González-Fernández, Á. Antibody-conjugated nanoparticles for biomedical applications. *J. Nanomater.* <https://doi.org/10.1155/2009/439389> (2009).
- Holford, T. R. J., Davis, F. & Higson, S. P. J. Recent trends in antibody based sensors. *Biosens. Bioelectron.* **34**, 12–24 (2012).
- Wingren, C. & Borrebaeck, C. A. K. Antibody Microarrays: Current Status and Key Technological Advances. *Omi. A J. Integr. Biol.* **10**, 411–427 (2006).
- Rusling, J. F., Kumar, C. V., Gutkinde, J. S. & Patele, V. Measurement of biomarker proteins for point-of-care early detection and monitoring of cancer. *Analyst* **135**, 2496–2511 (2010).
- Laia, G., Zhanga, H., Yong, J. & Yu, J. In situ deposition of gold nanoparticles on polydopamine functionalized silica nanosphere for ultrasensitive nonenzymatic electrochemical immunoassay. *Biosens Bioelectron.* **47**, 178–183 (2013).
- Yakoh, A., Pinyorosphum, C., Siangproh, W. & Chailapaku, O. Biomedical Probes Based on Inorganic Nanoparticles for Electrochemical and Optical Spectroscopy Applications. *Sensors* **15**, 21427–21477 (2015).
- Luppa, P. B., Sokoll, L. J. & Chan, D. W. Immunosensors—principles and applications to clinical chemistry. *Clin Chim Acta* **314**, 1–26 (2001).
- Ijeh, M. Covalent gold nanoparticle—antibody conjugates for sensitivity improvement in LFIA. (Mathematics, Informatics and Natural Sciences Faculty of Hamburg University, 2011).
- Ljungblad, J. Antibody-conjugated Gold Nanoparticles integrated in a Fluorescence based Biochip. (Department of Physics, Chemistry and Biology Linköpings Universitet, 2009).
- La Belle, J. T., Fairchild, A., Demirok, U. K. & Verma, A. Method for fabrication and verification of conjugated nanoparticle-antibody tuning elements for multiplexed electrochemical biosensors. *Methods* **61**, 39–51 (2013).
- He, X., Yuan, R., Chai, Y., Zhang, Y. & Shi, Y. A new antibody immobilization strategy based on electro-deposition of gold nanoparticles and Prussian Blue for label-free amperometric immunosensor. *Biotechnol. Lett.* **29**, 149–155 (2007).
- Khashayar, P. *et al.* Rapid prototyping of microfluidic chips using laser-cut double-sided tape for electrochemical biosensors Rapid prototyping of microfluidic chips using laser-cut double-sided tape for electrochemical biosensors. *J. Braz. Soc. Mech. Sci. Eng.* <https://doi.org/10.1007/s40430-016-0684-6> (2016).

13. Khashayar, P. *et al.* An Electrochemical Biosensor Based on AuNP-Modified Gold Electrodes for Selective Determination of Serum Levels of Osteocalcin, in *IEEE Sensors Journal* **17**(11), pp. 3367–3374 (2017).
14. Verma, H. N., Singh, P. & Chavan, R. M. Gold nanoparticle: synthesis and characterization. *Vet. World* **72**, 72–77 (2014).
15. Liu, X., Atwater, M., Wang, J. & Huo, Q. Extinction coefficient of gold nanoparticles with different sizes and different capping ligands. *Colloids Surfaces B Biointerfaces* **58**, 3–7 (2007).
16. Lai, G., Yan, F. & Ju, H. Dual Signal Amplification of Glucose Oxidase-Functionalized Nanocomposites as a Trace Label for Ultrasensitive Simultaneous Multiplexed Electrochemical Detection of Tumor Markers. *Anal. Chem.* **81**, 9730–9736 (2009).
17. Hu, M. *et al.* Gold nanostructures: engineering their plasmonic properties for biomedical applications. *Chem Soc Rev* **35**, 1084–1094 (2006).
18. Ackerson, C. J., Jadzinsky, P. D., Jensen, G. J. & Kornberg, R. D. Rigid, Specific, and Discrete Gold Nanoparticle/Antibody Conjugates. *J. Am. Chem. Soc.* **128**, 2635–2640 (2006).
19. Jazayeri, M. H., Amani, H., Pourfatollah, A. A., Pazoki-Toroudi, H. & Sedighmoghaddam, B. Various methods of gold nanoparticles (GNPs) conjugation to antibodies. *Sens. Bio-Sensing Res* **9**, 17–22 (2016).
20. Dixit, C. K., Vashist, S. K., MacCraith, B. D. & O’Kennedy, R. Multisubstrate-compatible ELISA procedures for rapid and high-sensitivity immunoassays. *Nat. Protoc.* **6**, 439–445 (2011).
21. Xia, N. *et al.* Probing of EDC/NHSS-Mediated Covalent Coupling Reaction by the Immobilization of Electrochemically Active Biomolecules. *Int. J. Electrochem. Sci* **8**, 2459–2467 (2013).
22. Raghav, R. & Srivastava, S. Immobilization strategy for enhancing sensitivity of immunosensors: L-Asparagine–AuNPs as a promising alternative of EDC–NHS activated citrate–AuNPs for antibody immobilization. *Biosens. Bioelectron* **78**, 396–403 (2016).
23. Rodriguez, I. A., Saxena, G., Hixon, K. R., Sell, S. A. & Bowlin, G. L. In vitro characterization of MG-63 osteoblast-like cells cultured on organic-inorganic lyophilized gelatin sponges for early bone healing. *J Biomed Mater Res Part A* **104**, 2011–2019 (2016).
24. Zhong, G., Liu, J. & Liu, X. A fast colourimetric assay for lead detection using label-free gold nanoparticles (AuNPs). *Micromachines* **6**, 462–472 (2015).
25. Guo, Z. *et al.* A molecular-gap device for specific determination of mercury ions. *Sci. Rep* **3**, 3115 (2013).
26. Day, E. S. *et al.* Antibody-conjugated gold-gold sulfide nanoparticles as multifunctional agents for imaging and therapy of breast cancer. *Int J Nanomedicine* **5**, 445–454 (2010).
27. Hunter, R. J. *Foundations of colloid science.* (Oxford University Press, 2000).
28. Henry, D. C. The Cataphoresis of Suspended Particles. Part I. The Equation of Cataphoresis. *Proc. R. Soc. London A Math. Phys. Eng. Sci* **133**, 106–129 (1931).
29. Lai, Y. H. *et al.* Rapid screening of antibody–antigen binding using dynamic light scattering (DLS) and gold nanoparticles. *Anal. Methods* **7**, 7249–7255 (2015).
30. Mihalescu, G. H., Olenic, L., Pruneanu, S., Bratu, I. & Kacso, I. The effect of pH on amino acids binding to gold nanoparticles. *J. Optoelectron. Adv. Mater.* **9**, 756–759 (2007).
31. Reverberi, R. & Reverberi, L. Factors affecting the Ag–Ab reaction. *Blood Transfus* **5**, 227–240 (2007).
32. Fischer, M. J. E. Amine Coupling Through EDC/NHS: A Practical Approach. *Methods Mol Biol* **627**, 55–73 (2010).
33. Hormozi-Nezhada, M. R., Seyedhosseinia, E. & Robotjazia, E. Spectrophotometric determination of glutathione and cysteine based on aggregation of colloidal gold nanoparticles. *Sci. Iran* **19**, 958–963 (2012).
34. Turkevich, J., Stevenson, P. C. & Hillier, J. A study of the nucleation and growth processes in the synthesis of colloidal gold. *Discuss. Faraday Soc* **11**, 55–75 (1951).
35. Frens, G. Controlled nucleation for the regulation of the particle size in monodisperse gold suspensions. *Nature* **241**, 20–22 (1973).
36. Basu, S. *et al.* Biomolecule induced nanoparticle aggregation: Effect of particle size on interparticle coupling. *J Colloid Interface Sci* **313**, 724–734 (2007).

Author Contributions

B.L. and J.V. made substantial contributions to conception and design of the study. P.K. performed the tests and wrote the main manuscript text. G.A., M.H. supervised the lab work. All authors reviewed the manuscript.

Additional Information

Competing Interests: The authors declare that they have no competing interests.

Publisher's note: Springer Nature remains neutral with regard to jurisdictional claims in published maps and institutional affiliations.



Open Access This article is licensed under a Creative Commons Attribution 4.0 International License, which permits use, sharing, adaptation, distribution and reproduction in any medium or format, as long as you give appropriate credit to the original author(s) and the source, provide a link to the Creative Commons license, and indicate if changes were made. The images or other third party material in this article are included in the article’s Creative Commons license, unless indicated otherwise in a credit line to the material. If material is not included in the article’s Creative Commons license and your intended use is not permitted by statutory regulation or exceeds the permitted use, you will need to obtain permission directly from the copyright holder. To view a copy of this license, visit <http://creativecommons.org/licenses/by/4.0/>.

© The Author(s) 2017